A Waveguide Impedance Meter for the Automatic Display of Complex Reflection Coefficient*

HENRY L. BACHMAN†

Summary—A waveguide impedance meter has been developed, comprising some specially designed components and some components previously designed for other applications. When this circuit is used in conjunction with the X-band rapid sweep oscillator and suitable display and control circuits, the impedance locus of a waveguide component is automatically and rapidly measured and oscillographically displayed in the reflection coefficient plane. A waveguide component having a $1\frac{1}{4}$-inch$\times\frac{5}{8}$-inch (large X-band) waveguide input port can be continuously measured throughout the frequency range extending from 8.5 to 9.6 kmc (12 per cent X-band). The bandwidth of the system is limited by the design bandwidth of the waveguide components. The plane of the impedance measurement may be referred to a plane internal to or external to the input port of the component under test. An expanded portion of the reflection coefficient plane may be displayed on the crt when small reflections are measured. The measurements of several representative impedances by the waveguide circuit were compared with slotted line measurements of these same components. For measurements of large reflections, standard ∞ db swr full scale display, the maximum observed errors of the magnitude and phase of the reflection coefficient as measured by the waveguide circuit were 10 per cent and 5 degrees respectively. These maximum errors occurred for measurements performed at the ends of the 12 per cent frequency band. The average errors of the magnitude and phase of the reflection coefficient were 2.5 per cent and 2 degrees respectively. For measurements of small reflections, with the crt display of the reflection coefficient plane expanded to 6 db swr full scale, the maximum observed deviation of the waveguide circuit measurements from slotted line measurements was 0.5 db swr, and the average deviation was 0.2 db swr. The maximum errors again occurred at the ends of the 12 per cent frequency band.

Introduction

THE complexity of modern waveguide systems, with the resulting requirements of components well-matched over broad bandwidths, requires an increasing amount of impedance data for the design and development of these components. The usual point-by-point method of measuring the frequency variations of the input impedance of microwave components, which requires the observation of the magnitude and phase of the standing wave ratio at each frequency and the plotting of this data on the reflection coefficient plane, can consume considerable time and effort. For this reason, the need for an instrument that would perform these measurements rapidly and automatically was recognized.

The waveguide impedance meter to be described was developed for use in conjunction with an X-band rapid sweep oscillator and suitable display and control circuits; the entire system is referred to as an automatic impedance plotter. This device provides for both the rapid automatic measurement of the input impedance variations of a waveguide component, and an oscillographic display of these variations in the reflection coefficient plane. Measurements may be performed continuously throughout the frequency range from 8.5 to 9.6 kmc (12 per cent X-band) on any microwave component having a $1\frac{1}{4}$-inch$\times\frac{5}{8}$-inch (large X-band) waveguide input port. Since the rapid sweep oscillator sweeps back and forth through the 12 per cent X-band at the rate of 12 cps, the cathode-ray tube display of the impedance locus is visually continuous. The speed of the measurement permits observations of changes in the impedance locus as the microwave component is adjusted, providing these adjustments are made at a speed slower than the frequency sweep rate (1/24 sec).

A photograph of the system appears in Fig. 1 (opposite page). At the extreme right is the X-band rapid sweep oscillator. The rf signal generated by the oscillator is fed into the input port of the waveguide impedance meter shown in the center of the photograph together with the crystal current bias circuit. The output signals of the waveguide circuit, which are at the modulation frequency of the rf oscillator, are fed into the amplifier channels of the display and control circuits; these circuits appear at the far left of the photo. The klystron power supply is not shown.

One feature of the oscillograph display is the ability to select any desired degree of expansion. The entire plane of the reflection coefficient (maximum radius equal to unity) may be presented; alternatively, some smaller radius may be chosen to expand the impedance locus for better observation of small reflections. By photographing the cathode-ray tube trace, a permanent record may be obtained.

A special feature of the waveguide circuit is the provision for choosing at will the reference plane, the plane at which the impedance is measured, simply by moving a short-circuiting plunger in a waveguide adjacent to the component under test. This permits the impedance locus to be observed at various planes either external to or within the component under test. This feature simplifies locating the best plane for the insertion of a matching device or for performing other studies of the impedance characteristics.

This paper is concerned almost entirely with a description of the waveguide impedance meter which was developed from both specially designed and already existing components. The X-band rapid sweep oscillator

* The subject of this paper was developed by the author for his Master's thesis at the Polytechnic Inst. of Bklyn., Brooklyn, N. Y.

† Wheeler Laboratories, Inc., Great Neck, N.Y.

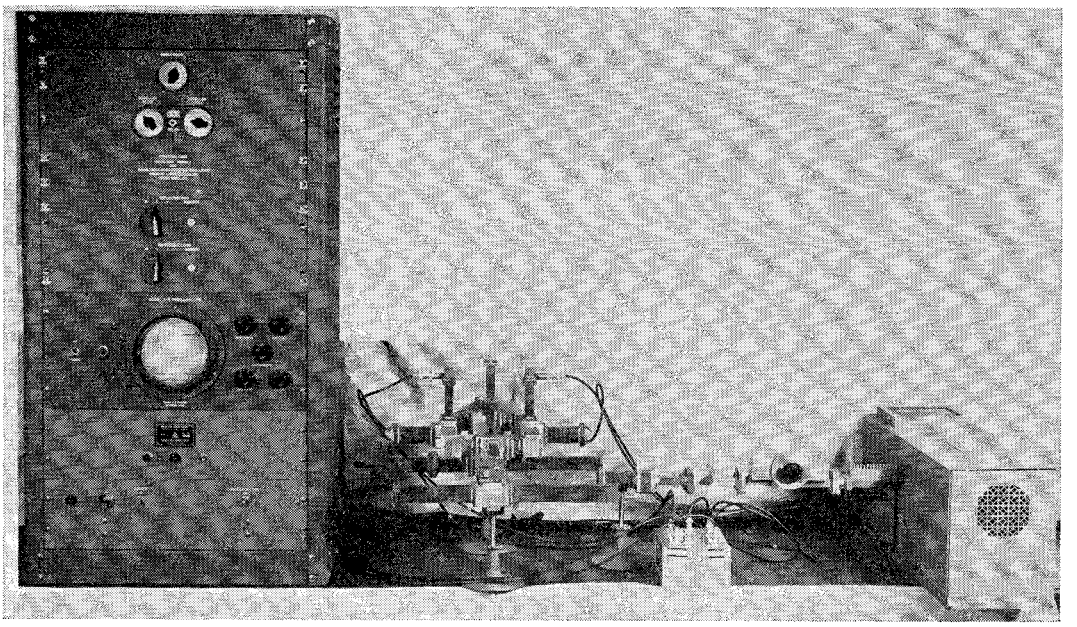

Fig. 1—Automatic impedance plotter.

and the display and control circuits were designed by Wheeler Laboratories for Bell Telephone Laboratories for another application.[1] The theory of operation of the waveguide circuit is first explained, and then the waveguide components comprising the waveguide network are described. Finally, an evaluation of the performance of the waveguide circuit and photographs of the results of measurements performed by the entire automatic impedance plotter system are given.

Theory of Operation

The impedance locus of a component with a varying parameter, such as frequency, may be plotted in the plane of the reflection coefficient. This type of plot has an advantage over a plot in the plane of the impedance, since all points of positive resistance are plotted within a circular area on the reflection coefficient plane. The polar form of the complex reflection coefficient $w = |w| \angle \beta$, can be described by the two orthogonal components, $|w| \cos \beta$ and $|w| \sin \beta$.

The waveguide impedance meter which is to be described generates signals proportional to these components when a test component having the complex reflection coefficient w is measured. The signals are amplified, detected and applied to the appropriate plates of the crt by means of the display and control circuits. The effect of these two signals is to trace on the face of the crt the impedance variation of the component in the reflection coefficient plane.

The principal component in the waveguide circuit, which will be referred to as the product detector, is shown schematically in Fig. 2. The product detector consists of a waveguide hybrid junction having one pair of conjugate ports (E-plane and H-plane) terminated in crystal detectors, and the other pair of conjugate ports (collinear) serving as signal input ports. The operation of this circuit remains essentially unchanged if the roles of each pair of conjugate ports are interchanged.

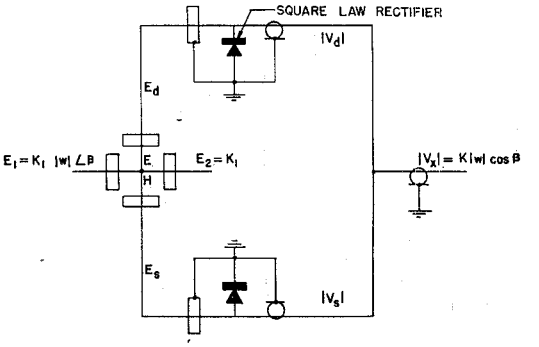

Fig. 2—Waveguide product detector circuit.

One complex input signal to the product detector, E_1, has a magnitude proportional to the voltage reflection coefficient of the test component and a phase, when referred to the other input signal, equal to that of the reflection coefficient. The other complex input signal, E_2, the reference signal, has a magnitude proportional to unity, the magnitude of the reflection coefficient of a short circuit. These two complex input signals are added and subtracted in the respective arms of the hybrid junction. The resulting sum and difference signals, E_s and E_d, are rectified and suitably combined (subtracted) to yield the product detector output signal, $|V_x|$. As is shown below, this signal is proportional to

[1] H. H. Rickert and D. Dettinger, "An X-band rapid sweep oscillator," IRE Convention Record, Part 10, "Instrumentation and Industrial Electronics," pp. 7–13.

the scalar product of the complex input signals; this result provides the basis for naming the circuit the product detector.

The complex electric fields at the collinear arms of the hybrid junction, which are modulated rf signals, are given as follows:

$$E_1 = K_1 |w| < \beta,$$
$$E_2 = K_1,$$

where $w = |w| \angle\beta$ is the complex voltage reflection coefficient of the test component placed at the appropriate port of the waveguide circuit. A multiplying factor e^{jwt}, indicating the sinusoidal time variation of the electromagnetic field, has been omitted in order to simplify the expressions. These input signals are added and subtracted in the H-plane and E-plane arms of the hybrid junction respectively, so that the complex electric fields in these arms are given by

$$E_s = \frac{1}{\sqrt{2}} [E_2 + E_1]$$
$$E_d = \frac{1}{\sqrt{2}} [E_2 - E_1].$$

The sum and difference signals, E_s and E_d, are detected in the crystal rectifiers. The magnitudes of the output voltages, $|V_s|$ and $|V_d|$, of the crystal rectifiers are proportional to the square of the magnitudes of the sum and difference signals if a square law response of the crystals is assumed. By the law of cosines,

$$|V_s| = K_2 |E_s|^2$$
$$= K_2 \left[\frac{|E_1|^2}{2} + \frac{|E_2|^2}{2} - |E_1 E_2| \cos (180° - \beta) \right]$$
$$= K_2 \left[\frac{|E_1|^2}{2} + \frac{|E_2|^2}{2} + |E_1 E_2| \cos \beta \right]$$
$$|V_d| = K_2 |E_d|^2$$
$$= K_2 \left[\frac{|E_1|^2}{2} + \frac{|E_2|^2}{2} - |E_1 E_2| \cos \beta \right],$$

where K_2 is the detection efficiency of each crystal detector, which is assumed equal for the two detectors. The relative phase of the detected voltages need not be considered.

Since one crystal has been reversed in the detector mount (cathode grounded), the magnitude of the product detector output voltage, which varies sinusoidally at the modulation frequency, is given by the difference of the detected sum and difference signals:

$$|V_x| = [|V_s| - |V_d|]$$
$$= 2K_2 |E_1 E_2| \cos \beta$$
$$= K |w| \cos \beta,$$

where all of the constants have been combined in K.

If either of the complex electric fields at the input to the product detector were shifted in phase by 90 degrees, the output of the product detector would then be given by

$$|V_y| = K |w| \cos (\beta \pm 90°)$$
$$= \pm K |w| \sin \beta.$$

When the output voltages, $|V_x|$ and $|V_y|$, of the two product detectors are suitably applied to each pair of deflection plates of an oscilloscope, the deflection of the spot on the crt will be proportional to the complex voltage reflection coefficient.

The above analysis has explained how the product detector operates to generate, from two definite input signals, the required output signals of the waveguide impedance meter. The remaining components of this circuit have the function of providing the proper signals to the product detector input ports. The complete waveguide circuit is shown schematically in Fig. 3.

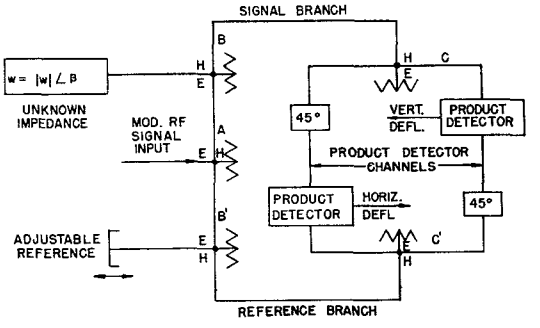

Fig. 3—Waveguide impedance meter.

The operation of the waveguide circuit is as follows. A square-wave modulated signal at the E-arm of hybrid junction A is divided equally into the two collinear arms, the H-arm (of this hybrid junction) being terminated in a matched load. (A simple E-plane "T" junction could have been used as a power divider, but this component does not have all of the desirable properties of the hybrid junction; namely, equal power split and isolation between the output arms.) The output signals of the collinear arms of hybrid junction A feed the signal and reference branches. The signals in these branches enter the E-arms of hybrid junctions B and B', where they are again divided equally into the collinear arms, while no signal enters the H-arm.

In hybrid junction B, in the signal branch, one collinear arm is terminated in a matched load, while the other arm is terminated with the component under test (unknown impedance). The signal in this collinear arm is reflected from the component under test by an amount dependent on the reflection coefficient of the component. The reflected signal, which is proportional to the reflection coefficient in magnitude and modified by the phase of the reflection coefficient, then divides equally into the E- and H-arms of the hybrid junction B. Only the signal at the H-arm of hybrid junction B

needs be considered, since to the first order, the signal at the E-arm is divided into the E- and H-arms of the hybrid junction A where it is absorbed. Similarly, the output of the H-arm of hybrid junction B', the collinear arms of which are terminated in a matched load and an adjustable short circuit, is proportional to the reflection coefficient of the short circuit, which is unity.

The magnitude of the signal at the input to the H-arm of hybrid junction C is then proportional to the magnitude of the reflection coefficient of the test component. Since the line lengths of the signal and reference branches are equal, the phase of this signal, relative to the phase of the signal at the input to the H-arm of hybrid junction C', is equal to the phase of the reflection coefficient of the test component. The magnitude of the signal at the H-arm of hybrid junction C' is proportional to unity. These signals, at the H-arms of hybrid junctions C and C', are equally divided into the collinear arms so that each product detector channel has one complex input signal with a magnitude proportional to the reflection coefficient of the component under test and a phase, referred to the other input signal, equal to the reflection coefficient; and one complex input signal with a magnitude proportional to unity.

It can be seen that the reference plane of the impedance measurement is determined by the position of the reference short circuit; it may be varied by changing the position of the short circuit. This procedure of referencing the plane of the impedance measurement to the plane of a short circuit is identical with the procedure employed when performing impedance measurements in the usual fashion on a slotted section.

The product detectors in Fig. 3 operate in exactly the manner as was previously described; however, the phase of the input signals has been modified. Instead of placing the 90-degree phase shift required in one of the product detector channels, this phase shift is divided equally between the two product detector channels by means of the two 45 degree phase shifters. This procedure, which provides symmetry of the waveguide circuit and simplifies the design of the phase shifter, still yields the 90-degree differential phase differences required between the phases of the product detector input signals. It can be easily shown, by the analysis previously employed, that the product detector output signals are only slightly modified, and have the following form:

$$|V_x| = K|w|\cos(\beta + 45°)$$
$$|V_y| = K|w|\sin(\beta + 45°).$$

These voltages, when suitably applied to the deflection plates of an oscilloscope, will be capable of plotting, on the face of the crt, the input impedance on the reflection coefficient plane in the same manner as the product detector output signals derived previously. The only difference will be that, in this case, the orthogonal axes of the reflection coefficient plane will be rotated 45 degrees relative to the axes of the deflection plates. The manner in which the proper beam deflection is obtained is shown in Fig. 4. The product detector output signals are amplified and detected by the display and control circuits before being applied to the plates of the oscilloscope.

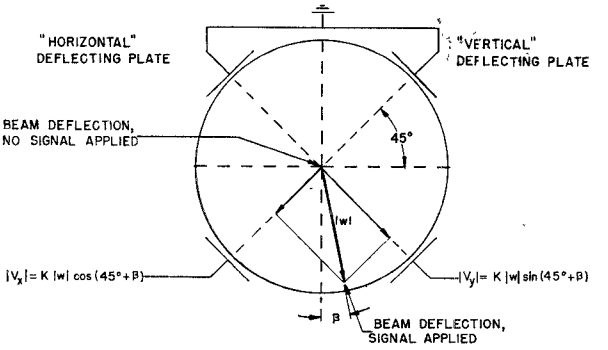

Fig. 4—Oscilloscope display.

It should be noted that in Fig. 4, as in all of the following data plotted in the reflection coefficient plane, a slightly modified form of the reflection coefficient plane is employed. The form used is that of the Wheeler Laboratories hemisphere chart.[2] This chart differs from the Smith and Carter charts of the reflection coefficient plane in the manner in which the axes are orientated. In the WL hemisphere chart, the vertical axis is the locus of pure resistance which increases from zero at the bottom to infinity at the top. To the right and left of this axis are plotted all values of impedance having a positive or negative reactive component respectively.

System Components

The waveguide impedance meter was developed partly from waveguide components specifically designed for use in this circuit, and partly from components which had been previously designed at Wheeler Laboratories for other applications.

Fig. 5 (next page) is a photograph of the waveguide circuit, comprising essentially all large X-band waveguide (RG-51/U) components. The rf signal input port is at the right-hand side of the photo between the two long matched load termination waveguides. The adjustable reference short circuit is shown at the left-hand side of the photo in the background. The waveguide port to which the component under test is connected appears in the left foreground of the photo. The ring circuit shown comprises the two product detector channels containing the phase shifters and the product detector hybrid junctions terminated at the E- and H-arm ports in crystal detectors. The detectors at the E-arm ports of the product detector hybrid junctions contain the 1N23B crystals, the detectors at the H-arm ports contain the 1N23BR (reversed) crystals. The crystal detector signals from the product detector hybrid junction

[2] H. A. Wheeler, "Wheeler Monographs," Monograph No. 4, Wheeler Labs.; 1953.

in the right side of the ring circuit are combined to yield the horizontal product detector output signal; the product detector in the left of the ring circuit provides the vertical product detector output signal.

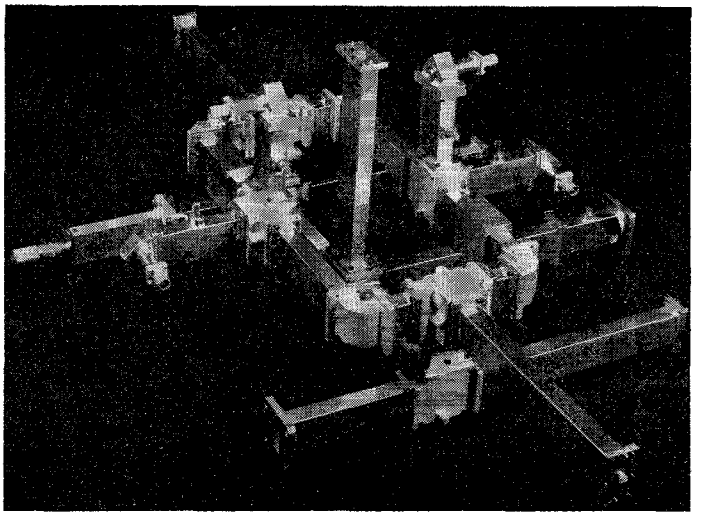

Fig. 5—Photograph of waveguide impedance meter.

The seven hybrid junctions in the waveguide circuit are production models of the WL X-band hybrid junction Model 201. These hybrid junctions are matched within 1.2 db swr in the H-arm, 1.0 db swr in the E-arm, and 1.2 db swr in each collinear arm over the 12 per cent X-band. The $E-H$-arm isolation, which is only a function of junction asymmetry, is better than 40 db; the collinear arm isolation, which is both a function of the junction asymmetry and the differences in match of the E- and H-arms, is better than 25 db.

The four detector mounts in the waveguide circuit are the WL Model 119 X-band single crystal mixer. Two of these detector mounts contain 1N23B crystal rectifiers, and the other two contain 1N23BR crystal rectifiers. The 1N23BR crystal is electrically equivalent to the 1N23B crystal; the mechanical configuration of the 1N23BR crystal has been arranged, so that it may be inserted in a reversed manner in the detector mount. The detectors were designed as broadband small-signal mixers; however, operating as detectors with 0.3 ma dc crystal current bias, they are matched to within 6 db swr over the 12 per cent X-band. The crystal current bias value was chosen as a compromise between the values yielding minimum detection conversion loss and least reflection.

To reduce the adverse effects of multiple reflections from the detectors on system operation, each detector is padded with a 7.5 db attenuator. This reduces the 6 db swr mismatch of the detectors to an apparent value of 1 db swr seen at the input to the pad. The pads consist of a $1\frac{3}{4}$-inch length of 200 Ω/sq irc resistance card, each end of which is tapered a distance of one-half wavelength to the waveguide height dimension. These lossy vanes are placed in the center of the waveguide parallel to the plane of the electric field vector. The mismatch of the detector pad is negligible compared to the mismatch of the detector.

The output of all four padded detectors is within .2 db. Because of the extremely low level signals existing at the crystal rectifiers (−15 dbm maximum), deviation from square law detection response is negligible.

The four 90-degree E-plane elbows which form a ring circuit of the two product detector channels are production models of the WL Model 226 90-degree double-mitered E-plane bend. These double-tuned bends are matched to within .15 db swr over the 12 per cent X-band.

Proper operation of the waveguide circuit requires two precision broad-band 45-degree phase shifters, and these components were designed specifically for use in the waveguide circuit. The simplest approach to the problem of obtaining a relative phase shift (difference in phase shift) of 45 degrees is to make the difference in length of the two waveguides comprising the phase shifter equal to $\lambda_g/8$ at the mid frequency; however, the relative phase shift would then deviate from 45 degrees by ±10 per cent over the 12 per cent X-band. This variation would have a detrimental effect on the operation of the waveguide circuit.

A novel method[3] has been employed to minimize the relative phase slope (change in phase difference with frequency) of the phase shifter. The relative phase slope, characteristic of waveguides having different lengths, is compensated by the reverse relative phase slope characteristic of two waveguides having different widths (cutoff frequency). This technique can best be described mathematically.

The relative phase shift ϕ between two waveguides of lengths l_1 and l_2 and cutoff frequencies f_1 and f_2 (guide wavelengths λ_{g1} and λ_{g2}), at a frequency f is given by

$$\phi = 2\pi\left[\frac{l_2}{\lambda_{g2}} - \frac{l_1}{\lambda_{g1}}\right]$$

$$= \frac{2\pi}{C}\left[l_2\sqrt{f^2 - f_2^2} - l_2\sqrt{f^2 - f_1^2}\,\right].$$

The first order change of the relative phase shift with frequency is given by

$$\frac{d\phi}{df} = \frac{2\pi f}{C}\left[\frac{l_2}{\sqrt{f^2 - f_2^2}} - \frac{l_1}{\sqrt{f^2 - f_1^2}}\right].$$

It is apparent, that the above expression for the phase slope will be zero, if

$$\frac{l_2}{\sqrt{f^2 - f_2^2}} = \frac{l_1}{\sqrt{f^2 - f_1^2}},$$

or, if

$$l_2\lambda_{g2} = l_1\lambda_{g1}.$$

[3] A. Sohon, "Wide-band phase-delay circuit," Proc. I.R.E., vol. 41, pp. 1050–1052; August, 1953.

For this condition, the relative phase shift is given by:

$$\phi = \frac{2\pi l_2}{C}\left[\frac{[f^2 - f_2^2] - [f^2 - f_1^2]}{\sqrt{f^2 - f_2^2}}\right].$$

At the design frequency (mid-frequency), for the appropriate values of the cutoff frequencies f_1 and f_2 of the waveguides, and the desired relative phase shift ϕ, the length of one waveguide, l_2, is calculated from the above expression. The length of the other waveguide, l_1, is then calculated from the expression required for the zero relative phase shift condition. It should be noted, that the condition for which the first derivative of ϕ with respect to frequency is zero, all other derivatives are not equal to zero. Therefore the technique will only eliminate the first order variation of relative phase shift with frequency. However, substantial improvement over the uncompensated condition does result.

For the design of the 45-degree phase shifters in the waveguide circuit, one waveguide was chosen to have large X-band waveguide cross-sectional dimensions, since this size waveguide (RG-51/U) is used throughout the remainder of the waveguide circuit. The other waveguide comprising the relative phase shifter was chosen to have a cutoff frequency which was close to the value of the cutoff frequency of large X-band waveguide, so that a negligible mismatch would result; but not so close that a prohibitive length would be required for the phase shifter waveguides. In addition, the aspect ratio of the cross-sectional dimensions of this special waveguide was made the same as the aspect ratio in large X-band waveguide, so that the mismatch of this guide would be minimized.

The design arrived at for the 45-degree phase shifters comprised a large X-band waveguide (1.122 inches $\times$0.497 inch inside dimension) 4.346 inches long, and a special fabricated waveguide 4.245 inches long with inside dimensions 1.073 inches$\times$0.475 inch. The relative phase shift was measured to be 45 degrees$\pm$0.2 degree over the 12 per cent X-band, and the special fabricated waveguide was matched to large X-band waveguide within 0.2 db swr over the band.

The reference short circuit in the reference channel of the waveguide circuit is the Waveline Model 561 waveguide adjustable short. This is a non-contacting short, equipped with a micrometer adjustment to provide accurate positioning of the reference plane. The total movement of 1 inch available makes it possible to vary the position of the reference plane by more than one-half guide wavelength at any frequency of operation. A special waveguide is provided at the port where the component under test is connected, so that, when the reference short circuit is in the mid-position of the available travel, the reference plane of the impedance measurement is at the plane of the input port of the component under test.

In order to preserve the isolation of the collinear arms of the power divider hybrid in the waveguide circuit, it is necessary that both the E- and H-arms of this hybrid be terminated in matched loads. Therefore, an attenuator is required at the input to the E-arm to pad the mismatch of the oscillator. Reduction of the 15 db mismatch of the oscillator to an apparent value of 0.2 db swr as seen from the E-arm of the hybrid requires a minimum attenuation of 18 db. This padding is accomplished by means of two 2-inch lengths of 200 Ω/sq irc resistance cards, each end of which is tapered a distance of one-half wavelength to the waveguide height dimension. Both carbon vanes are placed in the center of the waveguide parallel to the electric field vector, with the lossy surfaces exposed. Then, by displacing the two vanes one-quarter wavelength from each other along the center of the waveguide to cancel reflections from the taper edges, a match of better than 0.2 db swr over the 12 per cent X-band was obtained.

The five matched load terminations required were obtained by placing three vanes of 200 Ω/sq irc resistor cards in the waveguide parallel to the electric field vector. Each vane was tapered three wavelengths to the height dimension of the waveguide. One vane 10 inches long was placed in the center of the waveguide, and the other two, each one-quarter wavelength shorter, were displaced from the center of the waveguide to the position where the electric field has one-half the value at the center of the waveguide. With this arrangement, small reflections from the taper edges cancel, since the total reflection from the two side vanes is equal to the reflection from the center vane and is one-quarter wavelength out of phase with this reflection. The matched load terminations were matched to within 0.1 db swr over the 12 per cent X-band.

Performance

The accuracy of the waveguide impedance meter was determined independently of the entire automatic impedance plotter system, in order to eliminate the effects of errors caused by the display circuits and errors made in observation of the oscilloscope display. Evaluation of the performance of the waveguide circuit was made by comparing the results of impedance measurements performed by the waveguide circuit with slotted line measurements of the same microwave component.

The operation of the waveguide circuit was tested by measuring, at several discrete frequencies, the magnitude and sense of the product detector output voltages developed for a particular test component. The system was then calibrated at one frequency by measuring the voltages obtained with a component of known magnitude of reflection coefficient. The two product detector output voltages obtained for each frequency were then plotted on orthogonal axes on the reflection coefficient plane, and their vector sum obtained. The orthogonal axes represent the axes of each pair of deflection plates; they were rotated 45 degrees with respect to the real and imaginary axes of the reflection coefficient plane as was previously explained. The resultant vector sum of the two product detector output voltages yielded the com-

plex reflection coefficient in the reflection coefficient plane. The values of complex reflection coefficient obtained from the measurements of the product detector output voltages were then compared with the values determined from slotted line measurements of the test component at each frequency.

For testing the operation of the waveguide circuit with the full scale reflection coefficient chart ($|w|_{max}=1$ or ∞ db swr), the only true impedance standard available, the short circuit, was used as the test impedance. In the first test, this impedance was measured with the plane of the reference at the short circuit. Ideally, the resultant plot on the reflection coefficient plane is a point on the real axis corresponding to zero resistance for all frequencies. The resultant values of reflection coefficient as determined by the waveguide circuit are plotted in the reflection coefficient plane in Fig. 6. Twelve points were measured at 100 mc intervals from 8,500 to 9,600 mc. The system was calibrated to unity reflection coefficient at mid-band frequency (9,100 mc).

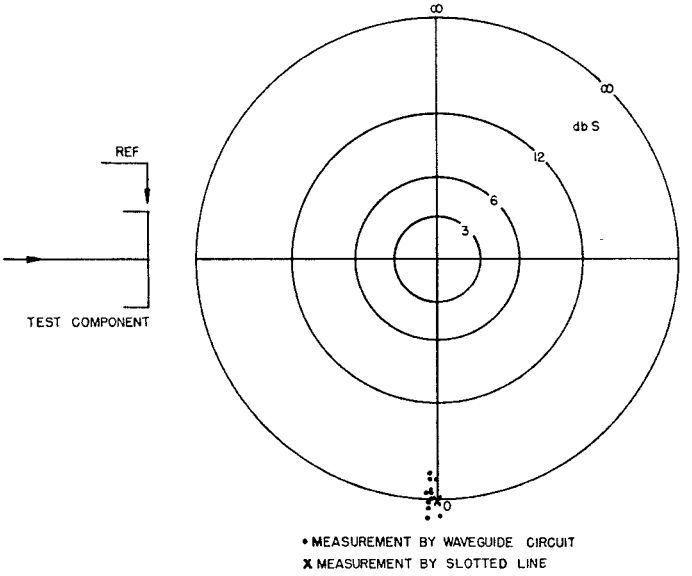

Fig. 6—Comparison of impedance measurements of short circuit.

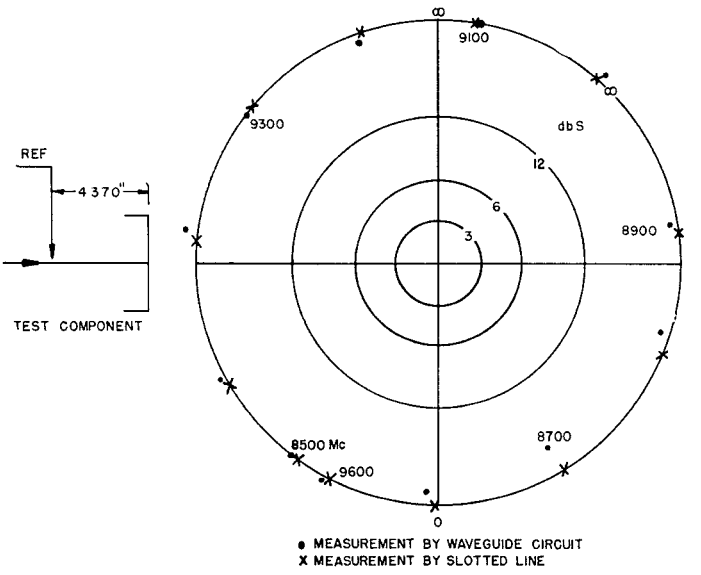

Fig. 7—Comparison of impedance measurements of short circuit.

The maximum errors observed for the magnitude and phase of the reflection coefficient were ± 10 per cent and 3 degrees respectively. As would be expected, these errors are a maximum at the ends of the band where the waveguide circuit components deviate the most from the ideal. The average errors observed for the magnitude and phase of the reflection coefficient were -2.5 per cent and 2 degrees respectively.

Since the product detector output voltages obtained for a short circuit impedance referenced at the plane of the short circuit were nearly constant at each frequency, the previous test was insensitive to errors that are dependent on the magnitude of these voltages. Therefore, another test was made with the short circuit impedance referenced far from the plane of the short circuit, so that the locus of the reflection coefficient forms one complete circle over the 12 per cent X-band. In this test, the product detector output voltages observed, vary over a dynamic range of 20 db.

The resultant values of reflection coefficient determined from the waveguide circuit are compared with slotted line measurements of this test impedance on the reflection coefficient plot in Fig. 7. Twelve points were measured at 100 mc intervals from 8,500 to 9,600 mc. The system was again calibrated at 9,100 mc. The maximum observed errors in magnitude and phase of the reflection coefficient were -10 per cent and 5 degrees respectively. As in the previous test, the maximum errors occur at the ends of the frequency band. The average observed errors in the magnitude and phase of the reflection coefficient were -1 per cent and 2 degrees respectively.

The final test to be described was made to determine the errors resulting from the use of an expanded display of the reflection coefficient plane. The display was expanded so that the full scale deflection correponded to 6 db swr reflection ($|w|_{max}=0.33$); such an expanded chart is used at Wheeler Laboratories.

Since there are no reliable standard mismatches available in the ranges of reflection coefficient appearing on the expanded display, the waveguide circuit was used to measure a single tuned circuit (thin resonant iris) terminated in a matched load; this impedance provided a dynamic range of product detector output voltages of 30 db. The results of the measurement performed on the waveguide circuit compared with slotted line measurements of the same impedance locus are plotted in the reflection coefficient plane in Fig. 8 (opposite page). The impedance measurement is referred to the plane of the iris. Twelve points were measured at 100 mc intervals from 8,500 to 9,600 mc. For this measurement, the waveguide circuit was calibrated at 9,100 mc with a 6 db swr mismatch

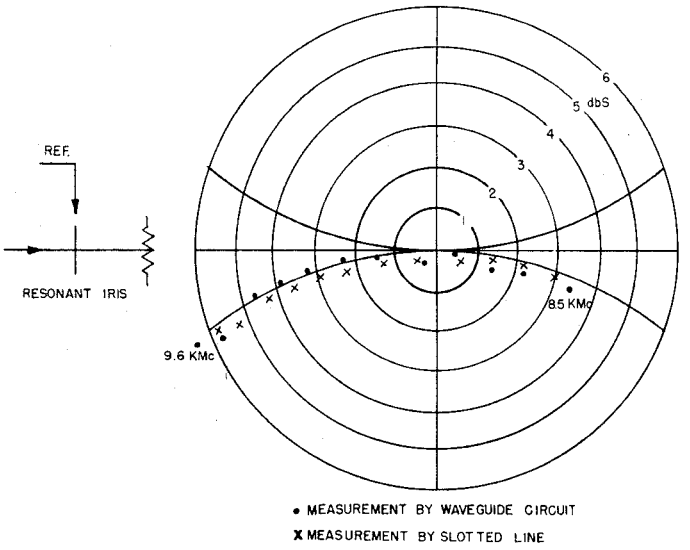

Fig. 8—Comparison of impedance measurements of tuned circuit.

obtained by padding a short circuit with a variable attenuator which was adjusted for a 6 db swr by a slotted line measurement. The results of the waveguide circuit measurement, in the worst case, differed by 0.5 db swr from the slotted line measurements. As in the previous tests, the maximum errors occur at the ends of the frequency band. The average deviation of the waveguide circuit measurement from the slotted line measurement was 0.2 db swr.

To illustrate the entire system performance, several representative test mismatches were automatically measured and the results displayed on the crt by the automatic impedance plotter.

Photographs of the resulting crt displays are shown in Figs. 9 and 10. The results of automatic impedance measurements of the test mismatches used in the waveguide circuit tests described above are given for purposes of comparison. The impedance locus of a short circui

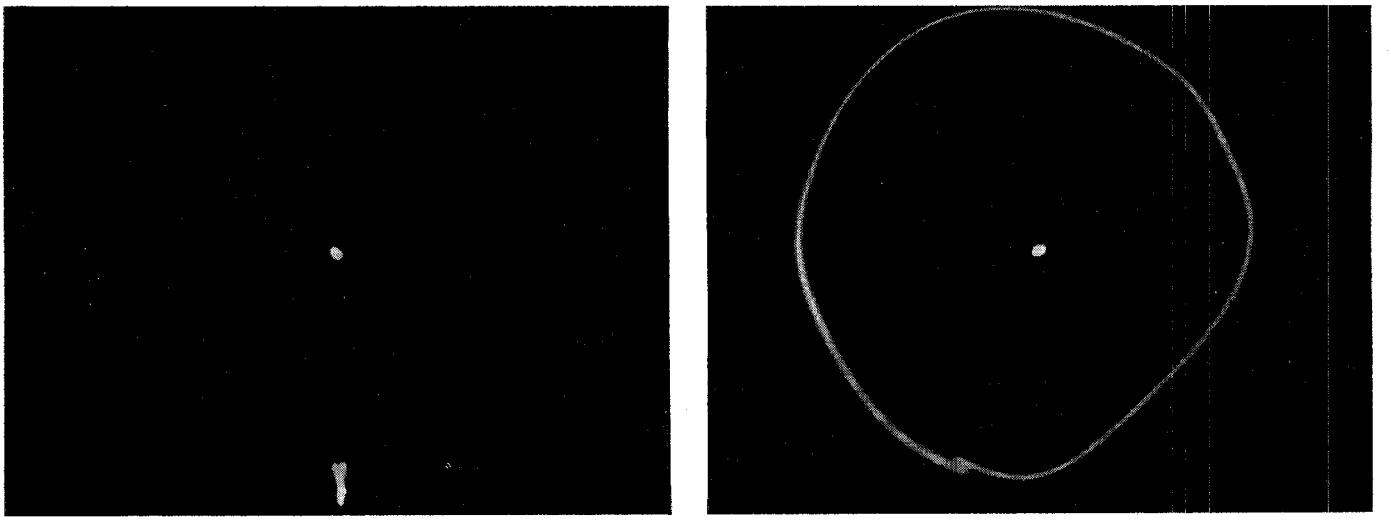

(a) (b)

Fig. 9—Photographs of impedance measurements of short circuit: (a) reference plane at short; (b) reference plane far from short.

(a) (b)

Fig. 10—Photographs of impedance measurements of tuned circuit: (a) single tuned; (b) multiple tuned.

measured with the plane of the reference at the short circuit is shown in Fig. 9(a). The measurement of the impedance locus of a short circuit referenced so as to give one complete circle on the reflection coefficient plane as the frequency is varied over the 12 per cent X-band is shown in Fig. 9(b). The display on the expanded reflection coefficient plane of the impedance locus of the single tuned circuit described above is shown in Fig. 10(a). Comparison of these photographs with the results yielded by the waveguide circuit alone (Figs. 6, 7, and 8) indicate that the accuracy of the entire system is essentially the same as the accuracy of the displays plotted from the output voltages of the waveguide circuit.

Finally, to further illustrate the usefulness of the automatic impedance plotter, a photograph of the expanded display resulting from the impedance measurement of a multiple-tuned waveguide filter circuit having a complex impedance locus is shown in Fig. 10(b). A measurement of this impedance locus by the usual slotted line techniques takes at least one hour; the measurement is performed instantaneously by the automatic impedance plotter following a setup time of about ten minutes. In addition, the measurement by the impedance plotter insures that all of the details of the impedance locus will be observed since the measurement is performed continuously over the frequency band.

It should be noted that in the photographs of the impedance plotter display, the crt trace at the center of each photo indicates the center of the reflection coefficient plane ($w=0$). The crt trace is returned to the center of the screen once during each frequency sweep cycle so as to indicate the impedance locus for the match condition.

A Method of Measuring Dissipative Four-Poles Based on a Modified Wheeler Network*

H. M. ALTSCHULER†

Summary—**A method of abstracting the parameters of dissipative four-poles from measured data is presented here. This semi-precision method is applicable to symmetric four-poles and results directly in a conveniently symmetric network representation. It is based on the modified Wheeler representation, a new and completely general network, which is introduced in this paper. In addition to the derivation of the network and of the analysis, the relationship that the network bears to its dual, to the impedance Tee, and to the admittance Ri is presented.**

Introduction

THE experimental procedures in four-pole measurements and the subsequent analyses of data can be divided roughly into two classes: "point" measurements on the one hand, and "precision" and "semi-precision" measurements on the other. While point measurements require that a specific and minimum number of datum points be taken and analyzed, precision and semi-precision measurements require that a sufficiently large number of different datum points are taken to be analyzed later by a technique which effectively averages them. In the latter class of measurements, which is of interest here, essentially two methods are available for measuring dissipative four-poles, as far as the author knows: the method due to Felsen and Oliner[1] and its variations, and Deschamps' method.[2]

It is pointed to note that, while the Felsen-Oliner networks are constituted of conventional network elements, they are not capable of displaying structural symmetry explicitly. The Deschamps method, in contrast, results in a scattering representation, and as such displays the symmetry (if any) of the measured structure explicitly, i.e., for symmetric structures, regardless of reference planes employed in the representation, $|S_{11}| = |S_{22}|$. It is apparent, then, that no precision or semi-precision measurement method has been available which *directly* results in a network (as opposed to a matrix representation) capable of representing symmetric structures in a symmetric fashion. To obtain such a network from precision or semi-precision measurements, it has been necessary to transform either the scattering representation or one of the Felsen-Oliner net-

* The work for this paper was conducted under Contract AF-19(604)-890 sponsored by the Air Force Cambridge Research Center.

† Microwave Research Institute, Polytechnic Institute of Brooklyn, Brooklyn, N.Y.

[1] L. B. Felsen and A. A. Oliner, "The Precision Measurement of Equivalent Circuit Parameters of Dissipative Microwave Structures," Report R-282-52, PIB-221, Polytechnic Inst. of B'klyn, Microwave Res. Inst.; November, 1952; also "Determination of equivalent circuit parameters for dissipative microwave structures," PROC. IRE, vol. 42, pp. 477–483; February, 1954.

[2] G. A. Deschamps, "Determination of reflection coefficients and insertion loss of a waveguide junction," *Jour. Appl. Phys.*, vol. 24, pp. 1046–1050; August, 1953.